Chinese Chemical Letters 33 (2022) 1051–1057

Contents lists available at ScienceDirect

Chinese Chemical Letters

journal homepage: www.elsevier.com/locate/cclet

Associative *vs.* dissociative mechanism: Electrocatalysis of nitric oxide to ammonia

Chaozheng He[a], Jia Wang[a], Ling Fu[b,*], Chenxu Zhao[a], Jinrong Huo[c]

[a] *Institute of Environment and Energy Catalysis, Shaanxi Key Laboratory of Optoelectronic Functional Materials and Devices, School of Materials Science and Chemical Engineering, Xi'an Technological University, Xi'an 710021, China*
[b] *College of Resources and Environmental Engineering, Tianshui Normal University, Tianshui 741001, China*
[c] *School of Sciences, Xi'an Technological University, Xi'an 710021, China*

ARTICLE INFO

Article history:
Received 8 August 2021
Revised 23 August 2021
Accepted 2 September 2021
Available online 8 September 2021

Keywords:
MBenes
Nitric oxide
NOER
First-principles calculation
Ammonia

ABSTRACT

Nitric oxide reduction to ammonia by electrocatalysis is the potential application in the elimination of smog and energy conversion. In this work, the feasibility of the application of two-dimensional metal borides (MBenes) in nitric oxide electroreduction reaction (NOER) was investigated through density functional theory calculations. Including the geometry and electronic structure of five kinds of MBenes, the adsorption of NO on the surface of these substrates, the selective adsorption of hydrogen protons during the hydrogenation process, and the overpotential in the electrocatalytic ammonia synthesis process. As a result, MnB exhibited the most favorable catalytic performance according to the associative pathways, which is thermodynamically performed spontaneously, and WB has a minimum overpotential of 0.37 V *vs.* RHE in the process of ammonia production according to the dissociative pathway. Overall, our work is the first to explore the electrocatalytic NO through the dissociative mechanism to synthesize ammonia in-depth and proves that MBenes are efficient NO electrocatalytic ammonia synthesis catalysts. These research results provide a new direction for the development of electrocatalytic ammonia synthesis experimentally and theoretically.

Nitric oxide (NO) is one of the main environmental pollutants produced by fossil combustion, which caused acid rain, ozone depletion, and photochemical smog [1]. In recent years, most countries have formulated quite strict policies to suppress NO emissions into the atmosphere [2,3]. Therefore, the conversion of NO to harmless substances including nitrate (NO_2^-), nitrogen (N_2) and ammonia (NH_3) is an effective way to make full use of nitrogen and reduce air pollution [4-6]. NH_3 is currently widely used in industry and agriculture. In industrial production, is converted to synthetic NH_3 using N_2 as a nitrogen source through the Haber-Bosch process resulting in high energy consumption and high pollution [7-9]. Although a more environmentally friendly and economical way named electrochemical nitrogen reduction (NRR) has received extensive attention [10-12]. However, since the strong inert nonpolar N≡N is difficult to be destroyed at room temperature, the current electrocatalytic synthesis of ammonia has multiple problems such as low NH_3 yield efficiency and poor selectivity of catalysis [13-15]. NO is another nitrogen-containing gas molecule, as a free radical which has an unpaired electron in the $2p^*$ antibonding orbital [16,17], thus the N–O bond is easy to activate. In recent years, some scholars have tried to use NO as a nitrogen source to synthesize ammonia through electrocatalysis which is named electrocatalytic nitric oxide electroreduction reaction (NOER).

Considering the diversity of NOER products, it is an important research direction that how to obtain nitrogen gas stably under a reasonable overpotential [18-20]. This also means that on the one hand, we must deepen our understanding of the catalytic mechanism, and on the other hand, we must find more efficient and stable catalysts [21-24].

In the past many years, there has been great interest in the noble metals which generally have excellent catalytic activity and rarely form oxides during the catalytic process [25-29], such as Pt [30], Cu [31], Au [32]. Jun Long and his coworkers combined DFT calculation and experiment to reveal the NOER process is more active than NRR and the electrochemical ammonia synthesis (EAS) reach to 517.1 μmol cm^{-2} h^{-1} when Cu is used as the catalyst [31]. Jing Yang studied NO reduction on Pt(111) surface by DFT calculation, during NO reduction to NH_4^+, HNO formation is more kinetic than NOH formation under different pathways [16]. However, the

* Corresponding author.
E-mail address: ful263@nenu.edu.cn (L. Fu).

https://doi.org/10.1016/j.cclet.2021.09.009
1001-8417/

noble pure metals currently used as NOER catalysts generally have the problem of high cost and low utilization rate. This situation makes it difficult for the existing catalysts to be used in large-scale industrial applications [33,34]. Therefore, we are motivated to discover more efficient and low-cost NOER catalysts.

Two-dimensional (2D) materials have been widely used in heterogeneous catalysis due to the wealth of unusual electronic structure and material properties [35-40]. For example, the Co-N_4 structure is embedded in graphene to construct a single-atom catalyst (SAC) [41-43], non-metallic NOER catalyst constructed with boron single atom doped two-dimensional graphene [44,45] and BC_2N nanotubes [46]. At the same time, the surface modification of two-dimensional materials such as MXenes is also generous in catalytic aspects [17,47-49]. In recent years, as a new type of two-dimensional material reported in theory and experiment, 2D transition metal borides (MBenes) which obtain by single crystals of the ternary borides have attracted widespread attention [50,51]. According to previous research, because of the co-existence of unoccupied and occupied d (p) states for the transition metal (boron) atoms [52,53], MBenes exhibited high stability and shown excellent performance in batteries and catalysis [47,54]. Guo *et al.* investigated seven kinds of MBenes applicated in electrocatalytic nitrogen reduction, which not only have limiting potentials range from -0.22 eV to -0.82 eV, but also can suppress the competitive hydrogen evolution reaction (HER) [55]. In addition to research on synthetic ammonia, MBenes have been found to have good performance in water splitting [51] and energy storage [56]. Inspired by the excellent performance of MBenes in catalysis and the difficulties currently faced by NOER. It is of great significance to study the application of MBenes to NOER.

In principle, the process of NO molecules catalyzing the synthesis of ammonia follows two mechanisms, association and dissociation, as NRR. When following the associative mechanism, NO molecules is adsorbed on the surface of catalyst, and the N–O bond is fully active but not broken. In the subsequent hydrogenation process of NO molecule, hydrogen protons and electrons selectively combine with N or O atoms to obtain different reaction intermediates. In the latter case, The N–O bond will be broken directly after adsorption, forming isolated N atoms and oxygen atoms on the surface of the catalyst, and then the N atoms and O atoms will be protonated to form NH_3 and H_2O, respectively.

In this work, we investigated the feasibility of MBenes (CrB, MnB, MoB, HfB and WB) for nitric oxide electrocatalytic synthesis of ammonia through density functional theory (DFT) calculations. Firstly, the mechanism of MBenes activation of NO molecules is analyzed by investigating the electronic structure of the NO adsorption states. Further studied the process of hydrogenation of NO to ammonia through the associative and dissociative mechanisms. The results show that all MBenes exhibit excellent catalytic property especially for MnB which can catalyze NO molecule to produce ammonia along with the associative mechanism spontaneously in thermodynamics.

All the computations were performed by using the Vienna ab initio simulation package (VASP) [57,58]. The Perdew Burke and Ernzerhof (PBE) functional within generalized gradient approximation (GGA) was used to describe the electronic exchange-correlation interaction [59,60]. The projector augmented-wave (PAW) method was applied to illustrate the interaction of ion-electrons [61]. Long-range dispersion interactions (DFT-D^3) of Grimme was invoked in all computation to describe the van der Waals interaction between intermediates and electrocatalysts [62]. Zero-point (ZPE) corrections were included to avoid the affection of the relative energy of competing reaction pathways [63]. The crystal orbital Hamilton populations (COHP) which is implemented in the LOBSTER code was used to analyze the chemical bonding between atoms [64].

According to our previous work, we select the 2D MBenes model were composed of 2 × 2 supercells (containing 8 boron and 8 transition metal atoms). To avoid artificial interactions, a vacuum of 15 Å was added in the *Z* direction [65]. The 5 × 5 × 1 Monkhorst-Pack was used to sample the Brillouin zone during geometry optimization and 7 × 7 × 1 k-points were applied to the electronic structure calculation. 500 eV plane-wave cut off energy was used for the basis set. The convergence tolerances for the energy were set as 10^{-5} and 0.02 eV/Å for the force, respectively. The Bader charge analysis was used to compute the charge transfer [66].

Adsorption energy (E_{ads}) of nitrogen oxide adsorb in 2D MBenes was calculated by the following equation [67]:

$$E_{ads} = E_{tot} - E_{Mbene} - E_{NO} \quad (1)$$

Where E_{tot} represents the total energy of the system adsorbed on 2D MBene by NO molecule. E_{MBene} and E_{NO} are the calculated energy of 2D MBene slab without adsorb species and the energy of nitrogen oxide in the gas phase, respectively. Specifically, if the adsorption energy E_{ads} is a positive value, it means that the adsorption of the NO molecule on the MBene surface is endothermic. On the contrary, if E_{ads} is a negative value, it means that the adsorption is a spontaneous process [68]. Generally speaking. While the adsorption energy exceeds -0.5 eV, it can be considered that NO is chemically adsorbed on the surface of MBenes.

According to the computational hydrogen electrode (CHE) model proposed by Nørskov [69,70]. Herein, the free energy ($H^+ + e^-$) of the electron-proton pair can be regarded as the chemical potential of 1/2 gaseous H_2 in equilibrium (0 V for standard hydrogen electrode). The Gibbs free energy between each electrocatalytic reaction step was obtained by the following equation [71]:

$$\Delta G = \Delta E + \Delta ZPE + T\Delta S + eU + \Delta G_{pH} \quad (2)$$

Where ΔE, ΔZPE and ΔS represent the adsorption energy, zero-point energy, and entropy at 298.15 K of the reaction intermediate on the substrate, respectively. The zero-point energies and entropies of the reaction intermediate were calculated through vibration frequencies, in which we fix the substrate and allow the absorb rate vibrational modes to be computed. ΔG_{pH} was calculated by $\Delta G_{pH} = k_B T \times pH \times \ln 10$, which is the free energy correction of pH, where k_B is the Boltzmann constant, and the value of pH is set to be 0 in our work. U and e were referred to the applied electrode potential and the number of electrons transferred in the whole reaction, respectively. Considering that the influence of the solvation effect in the whole reaction is less than 0.01 eV, we did not take it into account in the present work [72].

Combining previous theoretical calculations and experimental research results [17,73], we determined that MBenes are excellent electrocatalytic ammonia synthesis catalysts. There are many different crystal structures of MBenes. Herein, we only studied one of the structures (Figs. 1a and b) which is composed of two layers of atoms that transition metal atoms and boron atoms are alternately arranged. Each unit cell contains two transition atoms and two boron atoms with an orthorhombic group of *CMCM* [74]. The structure of MBenes determines that there will be four different adsorption sites for molecules which are marked T_M, T_{Boron}, Bridge and Hollow. Fig. 1c displays the electron localization function (ELF) of pristine CrB which indicates the covalent bond between B–B atoms and the ionic bond between Cr–B atoms. The more approach the ELF is at 0, the more obvious the delocalization of electrons, while ELF = 1 represents the electrons are completely localized. Significant charge accumulation can be observed around B atoms. This is because B atoms have higher electronegativity than Cr atoms, which causes electrons on Cr atoms to transfer to B atoms. At the same time, there is a layer of delocalized electrons on the surface

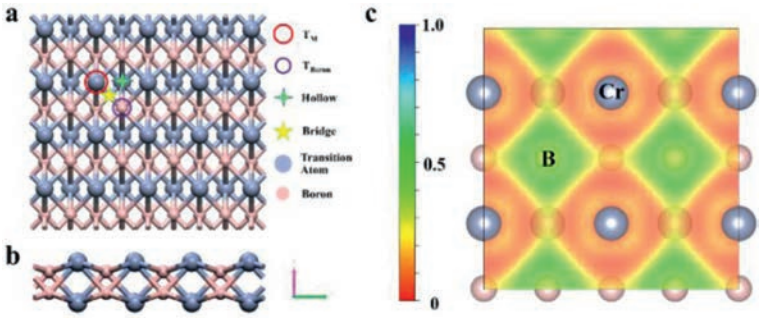

Fig. 1. (a, b) The structure and four possible active sites of the MBene. (c) Calculation electron localization function (ELF) of pristine CrB system.

of Cr atoms, which is a prominent feature of "electrene" materials [75]. Electrene materials can provide electrons during the catalysis process, which is a prerequisite for the effective catalysis of NO molecules.

The lattice parameters for five different MBenes are listed in Table S1 (Supporting information) which is sufficient geometric optimization. These dates indicate that the lattice parameters of MBenes are distributed between 2.87 Å and 3.10 Å, which means that the properties are similar. Table S2 (Supporting information) shows the top bond length between the B atom and the adjacent transition metal (TM) atom in the same layer and the adjacent B atom, respectively. For all the studied structures, the distance between the B atom and the transition metal atom is longer than the length of the B–B bond. The change in interatomic distance of MBenes is proportional to the change in the radius of transition metal atoms, indicating that MBenes are closely packed structures. It also shows the rationality of the model we built.

According to the principle of homogeneous catalysis, if nitric oxide is expected to be synthesized into ammonia by electrocatalysis, the catalyst is a prerequisite for its adsorption and activation [76]. We have discussed the adsorption of NO molecules on the above five positions. Compare with the nitrogen molecule, NO molecule has two adsorption configurations on the surface of MBenes: end-on and side-on. In the initial model building process, we only considered the downward chemical adsorption of the oxygen end on the surface of MBenes.

According to the structural characteristics of MBenes and previous research, we have established several adsorption structures including end-on and side-on adsorption structures. After sufficient geometric optimization, we have obtained the most stable NO adsorption structures on each MBenes surface which have the lowest energy. Table S3 (Supporting infromation) has listed these most stable structures of NO molecules' adsorption. The result has shown that all NO molecules tend to adsorb side-on configuration on MBenes. On the surface of MBenes, NO molecules are adsorbed at Hollow, except for the MoB surface which tends to be at Bridge. We calculated and measured the adsorption energy (E_{ads}) and the bond length (d_{NO}) of nitric oxide after activation on the surface of MBenes. Among them, the adsorption energy of CrB is -6.58 eV, and the corresponding NO molecular bond length is stretche.d to 1.27 Å. The lowest adsorption energy is MnB at -2.85 eV, and the corresponding NO molecular bond length is 1.26 Å. The adsorption energy of NO on the surface of MoB, HfB and WB is −4.43, −4.01 and −4.21 eV, respectively. The change in bond length also shows that these NO molecules are fully activated. Interestingly, the NO molecular bond length on the MoB surface is stretched to 1.40 Å, but the adsorption energy is not the maximum, which is caused by the adsorption of NO molecules on the MoB surface at the bridge sites. It indicates that the charge transfer between the B atom and the NO molecule promotes its activation.

To further analyze the NO adsorption situation. We also calculated the charge difference of these NO adsorption structures which is shown in Fig. 2. Cyan and yellow colors represent electron accumulation and depletion regions, respectively, with the isosurface value of 0.005 e/Å^3. As excellent "electrene" materials, all the MBenes contribute electrons to NO molecules in the process of catalyzing NO. Bader analysis further verified the process of charge transfer, and the results showed that the electrons obtained by NO molecules are contributed by transition metal atoms. This is consistent with the result of the qualitative analysis of charge differential. The charges contributed by transition metal atoms to NO molecules are 0.76 e$^-$ (CrB), 0.64 e$^-$ (MnB), 1.16 e$^-$ (MoB), 1.20 e$^-$ (HfB) and 0.91 e$^-$ (WB). The accumulation of negative charge on the surface of NO molecules is conducive to activating the N-O bond, which helps to promote the subsequent reactions.

Subsequently, we analyze the projected crystal orbital Hamilton populations (pCOHP) of nitric oxide after adsorption, which is shown in Fig. 3. To be consistent with previous research methods [77], we have drawn the positive contribution in the left named antibonding and the negative contribution in the right named bonding, which is marked as blue and red, respectively. It obviously that NO adsorb on a different surface of MBenes, there are several antibonding states close to the Fermi level, which is partially filled because the energy, at the same time, the bonding populations are below Fermi level and filled [78]. The more the antibonding orbital occupies, the higher the activation degree of the N-O bond. In contrast to isolated NO molecules, the $2\pi^*$ orbitals of the adsorbed NO molecules interact with the *d* orbitals of the metals, leading the $2\pi^*$ orbitals which near to Fermi Level split into occupied metal-bonding and unoccupied antibonding. Simultaneous, the 4σ, 1π and 5σ orbitals of the NO molecules adsorbed on the surface of MBenes hybridize with the 5s, 5p and 4d orbitals of the transition metals, and the 5σ orbitals spin density of the NO molecules increase [79,80]. We investigated the integrated crystal orbital Hamilton population (ICOHP) which can be deemed as the quantitative standard of NO activation degree. The positive value of ICOHP represents the anti-bond of the atomic bond, and the negative value represents the bond between atoms. The more negative the value presents the stronger bonding between the two atoms. Fig. 3f shows the number of electrons transferred N_e and corresponding ICOHP value for different MBenes. This linear correlation quantitatively explains the effect of the amount of charge transfer on the activation of nitric oxide molecule bonds [77]. The more quantity of charge transferred from MBenes to the NO molecule, the weaker the interaction between nitrogen and oxygen which represents the higher the degree of activation. The result shows that the NO activation degree on the surface of MoB is the best advantage, while the NO activation degree on the surface of MnB is the lowest. This result is also corresponding with our previous

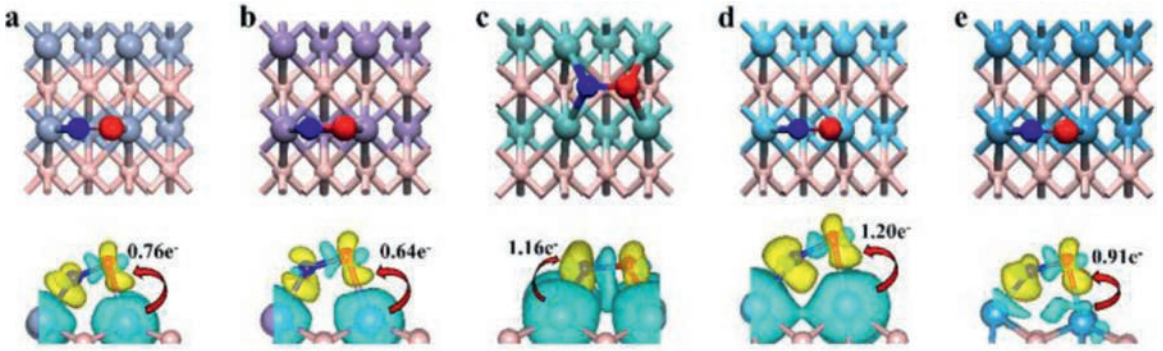

Fig. 2. The top view is the most stable NO molecule structure adsorbed on the surface of MBenes, and the side view is the corresponding charge difference. (a) CrB-NO, (b) MnB-NO, (c) MoB-NO, (d) HfB-NO, (e) WB-NO. Bule and red balls represent nitrogen and oxygen atom, respectively. The corresponding figure below the adsorption structure is the corresponding charge difference. Cyan and yellow colors represent electron depletion and accumulation regions, respectively, with the isosurface value of 0.005 e/Å^3.

differential charge and Bader charges analysis results which indicating that MoB has the best effect on activating NO molecules.

After determining the best adsorption structure for NO on different MBenes, we further research the electrocatalytic reduction of NO to ammonia. The overall reaction is $NO(g) + 2H^+ + 5e^- \rightarrow NH_3(g) + H_2O(l)$, considering that the purpose of our research is to synthesize ammonia from nitric oxide, the electrocatalytic process is terminated when ammonia is produced. The possible NOER pathways (associative and dissociative) have been considered and shown in Fig. S1 (Supporting information). In this research, the reaction equations of the associative and dissociative mechanism are corresponding to the following:

$$^*NO + 4H^+ + 4e^- \rightarrow {}^*NH_3 + {}^*OH \quad (3)$$

$$^*NO + 3H^+ + 3e^- \rightarrow {}^*NH_3 + {}^*O \quad (4)$$

While the N-O molecule adsorbs on the surface of MBenes with a side-on configuration, it will be hydrogenated to synthesize NH_3 along two different pathways of associative and dissociative during the hydrogenation process. When synthesizing ammonia along the dissociation path, the NO bond is broken after adsorption, and isolated nitrogen and oxygen atoms are formed on the surface of MBenes. Subsequently, the separated nitrogen atoms can obtain $H^+ + e^-$ from the electrolyte and undergo a hydrogenation reaction until ammonia gas is produced. As for the associate pathway, when the $H^+ + e^-$ are approaching the adsorbed NO molecule. It is necessary to calculate the adsorption barrier to determine the binding site of the H proton and confirm the formation of *NOH or *NHO. With the change of the H proton binding site in each step, the product produced also changes. Therefore, the pathway taken by different catalysts to produce ammonia is different.

The Gibbs free profiles of NO hydrogenation to NH_3 on the surface of CrB and MnB have been shown in Figs. 4a and b. For the molecule on the surface of CrB and MnB, the limiting step for both are *NO → *N + *O, and the corresponding overpotential according to the dissociative pathway is 1.67 and 3.06 eV, respectively. When NO molecules dissociate on the surface of CrB and MnB, the hydrogenation of N atom to form NH_3 according to the formula $^*N + 3H^+ + 3e^- \rightarrow NH_3$, In the subsequent process, $^*NH_2$

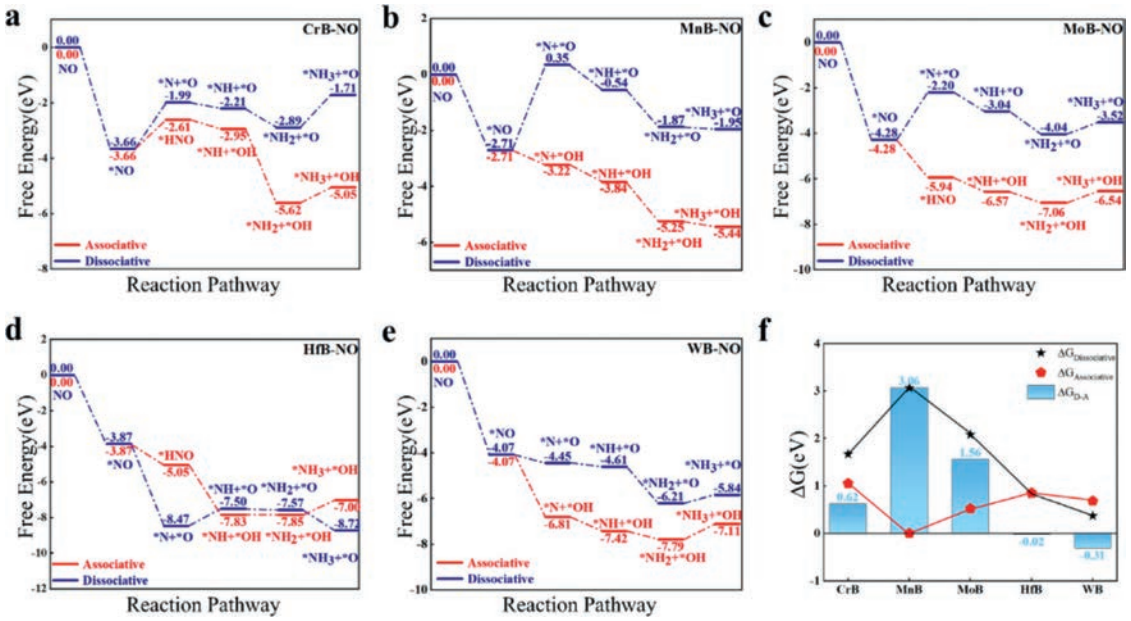

Fig. 4. Free-energy diagrams of ammonia synthesis with the lowest energy through associative and dissociative pathways after the adsorption of NO on (a) CrB, (b) MnB, (c) MoB, (d) HfB and (e) WB, respectively. (f) The limiting energy of different substrates hydrogenates NO molecules to ammonia according to dissociative and associative mechanisms, $\Delta G_{D\text{-}A}$ represents the free energy difference of the rate-limiting steps corresponding the dissociative mechanism and the association mechanism.

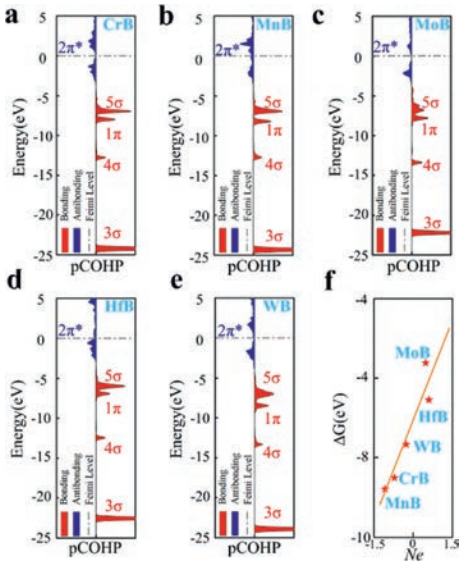

Fig. 3. (a-e) The projected crystal orbital Hamilton populations (pCOHP) between the nitrogen atom and oxygen atom after NO molecule adsorbed on the surface of MBenes, where red represents bonding and blue represents antibonding. (f) Illustration of the correlation between the adsorption energy of nitric oxide and the integrated COHP (ICOHP).

on the surface of CrB needs to overturn a barrier about 1.18 eV when obtaining hydrogen protons and electrons to form NH_3. On the contrary, the hydrogenation of isolated N atoms on the surface of MnB until ammonia synthesis is a spontaneous process. Fig. S2 (Supporting information) has exhibited the geometrically optimized structure of the intermediates. As for NO on the CrB to synthesize ammonia along with associative mechanism, the NO molecule captures the first hydrogen proton and combines with the N atom to form *NHO which needs to consume the energy of about 1.05 eV. It is the advantage to combine with the O atom to form *OH when the second hydrogen proton reaches to *NHO. In the subsequent reaction, H protons and electrons gradually combine with the N atom until the generated ammonia gas and escaped from the surface of CrB, which is exothermic. The entire process of hydrogenation for NO on the surface of MnB to produce ammonia along the associative pathway is exothermic, which means that it can occur spontaneously in terms of thermodynamics. Combining Fig. 4b and Fig. S3 (Supporting information), the formation of *OH on the surface of MnB is more advantageous than *HNO, and the N-O bond is broken after *OH is produced. Surprisingly, the process of hydrogenation of NO molecules on the surface of MnB to ammonia along the associative pathway is completely thermodynamically spontaneous.

The free energy diagram of NO hydrogenation to synthesize ammonia on the surface of MoB is displayed in Fig. 4c. The two processions of $^*NO \rightarrow {}^*N + {}^*O$ and $^*NH_2 + {}^*O + H^+ + e^- \rightarrow {}^*NH_3 + {}^*O$ need to adsorb 2.08 and 0.52 eV of energy from the electrode when the NOER process along the dissociative pathway. Fig. S4 (Supporting information) is the optimized structure diagram of the corresponding intermediates. In contrast, the energy required for direct hydrogenation without dissociation of NO molecules is lower. The hydrogen atom combines with the nitrogen atom to form *NHO and the bond of N–O is stretched which is a spontaneous process. Subsequently, the second hydrogen atom will be adsorbed on the oxygen atom, breaking the N–O bond and forming *OH which has a direction and angle similar to *NH. Ammonia is first generated instead of water until the end of the reaction which is accompanied by the energy consumption of 0.52 eV in the process of $^*NH_2 + {}^*O + H^+ + e^- \rightarrow {}^*NH_3 + {}^*O$. For HfB catalyze NO molecules, no matter whether the NO bond breaks or hydrogenation occurs firstly, it can proceed spontaneously. The change of the free energy of NO reduction (Fig. 4d) indicating that the corresponding overpotentials for the associative and dissociative pathways are 0.85 and 0.83 eV, respectively. As shown in Fig. S5 (Supporting information), hydrogen molecules are first combined with nitrogen atoms to form *NHO according to the associative pathway. Nitrogen and oxygen are separated after the second hydrogen combine to produce *OH and *NH and the limiting step is $^*NH_2 + {}^*OH + H^+ + e^- \rightarrow {}^*NH_3 + {}^*OH$ in the whole reaction. When the NO molecule dissociates in the first step, the limiting step is $^*N + {}^*O + H^+ + e^- \rightarrow {}^*NH + {}^*O$ which is continuously exothermic in the subsequent hydrogenation reaction. The NOER process of NO molecule adsorbs on the WB surface is shown in Fig. 4e. The hydrogenation processes are all exothermic and spontaneously proceed except for the final step of generating ammonia gas for the associative and dissociative pathways. Limiting step of the associative and dissociative pathway are $^*NH_2 + {}^*OH + H^+ + e^- \rightarrow {}^*NH_3 + {}^*OH$ and $^*NH_2 + {}^*O + H^+ + e^- \rightarrow {}^*NH_3 + {}^*O$, and the corresponding overpotentials are 0.68 and 0.37 eV, respectively. Fig. S6 (Supporting information) is the geometrically optimized structure of the intermediates. Under the associative pathway, the first hydrogen proton combined with the adsorbed NO molecule is more likely to adsorb on the oxygen atom to break the N-O bond and form a hydroxyl group. The hydroxyl group accompanies by subsequent reactions until ammonia is produced.

Although many researchers are dedicated to finding suitable catalysts to improve the performance of the electrocatalytic synthesis of ammonia through N_2 molecules, due to the high bond energy (942 kJ/mol) and low solubility in aqueous solutions of N_2 molecules, making the actual industrial application is more difficult. As shown in Table S4 (Supporting information), in the process of N_2 synthesis of ammonia, the hydrogenation of the first N_2 molecule, that is, the breaking of the first bond is often a critical step that limits the entire reaction. NO molecule as an environmental pollutant contains free radicals and high chemically reactive. As a nitrogen source for synthetic ammonia, not only can reduce the difficulty of the reaction but also reduce environmental pollution which has more advantages than N_2 molecules. Table S5 in Supporting Information list the NOER performance of various electrocatalysts in previous research. They focused on the reports that NO molecules produce ammonia along with the associative mechanism instead of the dissociative mechanism.

We summarized the overpotential of nitric oxide electrocatalytic synthesis of ammonia on the surface of five MBenes by different mechanisms in Fig. 4f. Among them, the electrocatalytic reduction of NO by CrB, MnB and MoB is more inclined to the associative pathway, while the dissociative pathway of HfB and WB is more favorable. For the associative pathway, NO can be completely spontaneously hydrogenated to synthesize ammonia thermodynamically on the surface of MnB. According to the experimental research of Long *et al.* [31], copper is the best pure metal catalyst for NOER due to its moderate catalytic activity and its overpotential is 0.9 V *vs.* RHE. Our results show that, except for CrB (1.05 eV), all other MBenes require a lower overpotential than Cu during the NOER process which means MBenes are more suitable catalysts for NOER reaction. And for the dissociative pathway, the overpotential for NO dissociation on the surface of CrB, HfB, and WB is less than 0.7 eV which is feasible in actual production. This mechanism has not been reported in previous studies, and it can guide for theoretical and experimental workers to analyze the NOER mechanism in depth.

According to previous research results, MBenes exhibit excellent performance as electrocatalytic catalysts for the synthesis of ammonia from NO. In the process of NO molecule adsorption, MoB exhibits the optimal activation performance for NO molecules which surpasses other substrates. Combined with the analysis of the electronic structure, we found that the unique adsorption structure of NO on the surface of MoB is more favorable for transferring charges to the NO molecule. In the subsequent hydrogenation reaction of the NO molecule, the NO molecule on the surface of MoB produces ammonia along with the associative mechanism, which can proceed spontaneously in thermodynamics. However, from the perspective of the overpotential in the entire reaction process, MnB, as the substrate with the most disadvantage activation effect on NO molecules, can spontaneously synthesize ammonia from NO along with the associative mechanism. According to the Brønsted–Evans–Polanyi (BEP) relation [81], the activation effect of the substrate on small molecules is inversely proportional to the dissociation barrier of NH_x, which leads to the need to overcome the energy barrier for the desorption of NH_3 generated on the surface of MoB. Simultaneously, the poor activation of NO results in the dissociative energy barrier of NO molecule on the surface of MnB as high as 3.06 eV, which becomes the main factor for the synthesis of ammonia according to the dissociative mechanism. Both the dissociation and the association mechanism are excellent when NO molecules are hydrogenated on the surface of WB to produce ammonia. In general, since NO molecules are more easily activated than N_2, when it is used as a nitrogen source to produce ammonia, choosing a catalyst with too good or too poor catalytic activity may lead to an increase in energy consumption of the reaction. At the same time, in the process of experiment and industrial production, it is difficult for us to control the actual reaction mechanism. Thus it is extremely important to choose a catalyst with a moderate activation performance for NO molecules.

In summary, based on density functional theory calculations, we investigated the possibility of 2D MBenes (CrB, MnB, MoB, HfB and WB) electrocatalysis for NO synthesis ammonia. On the surface of these materials, the different adsorption configurations of NO on four different adsorption sites have been studied. All NO is adsorbed on the surface of MBenes with a side-on configuration as the most stable structures after geometric optimization. The electron density difference and projected crystal orbital Hamilton populations have given an in-depth analysis of the activation mechanism of NO molecules. Subsequently, the process of hydrogenation of activated NO molecules to NH_3 through association and dissociation pathways was explored. The overpotentials of the association and dissociation pathways are 0 and 0.37eV which are corresponding to MnB and WB, respectively. The result of our research provides guidance for the application of 2D MBenes in the field of electrocatalysis and promoted the development of new experiments and theoretical synthesis of ammonia.

Declaration of competing interest

The authors declare that they have no known competing for financial interests or personal relationships that could have appeared to influence the work reported in this paper.

Acknowledgments

This study was funded by the Natural Science Foundation of China (No. 21603109), the Henan Joint Fund of the National Natural Science Foundation of China (No. U1404216), the Special Fund of Tianshui Normal University, China (No. CXJ2020-08), and the Scientific Research Program Funded by Shaanxi Provincial Education Department (No. 20JK0676).

Supplementary materials

Supplementary material associated with this article can be found, in the online version, at doi:10.1016/j.cclet.2021.09.009.

References

[1] S. Zhang, D. Chen, Z. Liu, et al., Appl. Catal. B 284 (2021) 119686.
[2] P. Granger, V.I. Parvulescu, Chem. Rev. 111 (2011) 3155–3207.
[3] F. Rao, G. Zhu, W. Zhang, et al., ACS Catal. 11 (2021) 7735–7749.
[4] Z. Ma, L. Sheng, X. Wang, et al., Adv. Mater. 31 (2019) e1903719.
[5] Y. Wang, M. Batmunkh, H. Mao, et al., Chin. Chem. Lett. (2021), doi:10.1016/j.cclet.2021.05.025.
[6] S. Zhou, K. Chen, J. Huang, et al., Appl. Catal. B 266 (2020) 118513.
[7] M. Reiners, D. Baabe, K. Munster, et al., Nat. Chem. 12 (2020) 740–746.
[8] R. Wang, C. He, W. Chen, et al., Chin. Chem. Lett. 32 (2021) 3821–3824.
[9] X. Lv, W. Wei, B. Huang, et al., Nano Lett. 21 (2021) 1871–1878.
[10] W. Zhao, L. Zhang, Q. Luo, et al., ACS Catal. 9 (2019) 3419–3425.
[11] G. Xu, H. Li, A.S.R. Bati, et al., J. Mater. Chem. A 8 (2020) 15875–15883.
[12] X. Lv, W. Wei, F. Li, et al., Nano Lett. 19 (2019) 6391–6399.
[13] Z.W. Seh, J. Kibsgaard, C.F. Dickens, et al., Science 355 (2017) eaad4998.
[14] G.F. Chen, S. Ren, L. Zhang, et al., Small Methods 3 (2018) 1800337.
[15] W. Xu, G. Fan, J. Chen, et al., Angew. Chem. Int. Ed. 59 (2020) 3511–3516.
[16] J. Yang, Phys. Chem. Chem. Phys. 21 (2019) 6112–6125.
[17] J. Wang, C. He, J. Huo, et al., Adv. Theory Simul. 4 (2021) 2100003.
[18] M.M. Mason, Z.R. Lee, M. Vasiliu, et al., ACS Catal. 10 (2020) 13918–13931.
[19] F. Rao, G. Zhu, W. Zhang, et al., Appl. Catal. B 281 (2021) 119481.
[20] R. Sun, C. He, L. Fu, et al., Chin. Chem. Lett. (2021), doi:10.1016/j.cclet.2021.05.072.
[21] S. Deshpande, J. Greeley, ACS Catal 10 (2020) 9320–9327.
[22] H. Lei, M. Wu, F. Mo, et al., Environ. Sci. Nano 8 (2021) 1398–1407.
[23] W. Wu, Z. Ao, T. Wang, et al., Phys. Chem. Chem. Phys. 16 (2014) 16588–16594.
[24] C. Cao, D.-D. Ma, J. Jia, et al., Adv. Mater. 33 (2021) 2008631.
[25] J. Han, S. Zhang, Q. Song, et al., Sustain. Energy Fuels 5 (2021) 509–517.
[26] S. Zhang, B. Zhang, D. Chen, et al., Nano Energy 79 (2021) 105485.
[27] Y. Sun, Y. Wang, H. Li, et al., J. Energy Chem. 62 (2021) 51–70.
[28] J. Chen, H. Lei, S. Ji, et al., J. Colloid Interface Sci. 601 (2021) 704–713.
[29] D.D. Ma, S.G. Han, C. Cao, et al., Energy Environ. Sci. 14 (2021) 1544–1552.
[30] H.J. Chun, V. Apaja, A. Clayborne, et al., ACS Catal. 7 (2017) 3869–3882.
[31] J. Long, S. Chen, Y. Zhang, et al., Angew. Chem. Int. Ed. 59 (2020) 9711–9718.
[32] J. Choi, H.L. Du, C.K. Nguyen, et al., ACS Energy Lett. 5 (2020) 2095–2097.
[33] J.R. Huo, J. Wang, H.Y. Yang, C.Z. He, J. Mol. Model 27 (2021) 38.
[34] Y.L. Wu, X. Li, Y.S. Wei, et al., Adv. Mater. 33 (2021) 2006965.
[35] S.Z. Butler, S.M. Hollen, L. Cao, et al., ACS Nano 7 (2013) 2898–2926.
[36] W.J. Yang, Z.Y. Gao, X.S. Liu, et al., Fuel 243 (2019) 262–270.
[37] L.R. Johnson, S. Sridhar, L. Zhang, et al., ACS Catal. 10 (2019) 253–264.
[38] L. Wang, X. Shi, Y. Jia, et al., Chin. Chem. Lett. 32 (2021) 1869–1878.
[39] H. Lei, M. Wu, Y. Liu, et al., Chin. Chem. Lett. 32 (2021) 2317–2321.
[40] S. Gong, G. Zhu, R. Wang, et al., Appl. Catal. B 297 (2021) 120413.
[41] G. Liu, J. Zhou, W. Zhao, et al., Chin. Chem. Lett. 31 (2020) 1966–1969.
[42] P. Chen, Y. Huang, Z. Shi, et al., Materials 14 (2021) 2469.
[43] H. Zhang, W. Wei, S. Wang, et al., J. Mater. Chem. A 9 (2021) 4082–4090.
[44] S. Ji, J.X. Zhao, New J. Chem. 42 (2018) 16346–16353.
[45] X. Chen, W.J. Ong, Z. Kong, et al., Sci. Bull. 65 (2020) 45–54.
[46] Y.Q. Liu, C. Liu, A. Kumar, Mol. Phys. 118 (2020) e1798528.
[47] W. Song, J. Wang, L. Fu, et al., Chin. Chem. Lett. 32 (2021) 3137–3142.
[48] N. Li, J. Peng, W.J. Ong, et al., Matter 4 (2021) 377–407.
[49] Z. Zeng, X. Chen, K. Weng, et al., NPJ Comput. Mater. 7 (2021) 80.
[50] M. Ade, H. Hillebrecht, Inorg. Chem. 54 (2015) 6122–6135.
[51] T. Zhang, B. Zhang, Q. Peng, et al., J. Mater. Chem. A 9 (2021) 433–441.
[52] X. Yang, C. Shang, S. Zhou, J. Zhao, Nanoscale Horiz 5 (2020) 1106–1115.
[53] Y. Sun, Z. Deng, X.-M. Song, et al., Nanomicro. Lett. 12 (2020) 133.
[54] T. Bo, P.F. Liu, J. Xu, et al., Phys. Chem. Chem. Phys. 20 (2018) 22168–22178.
[55] X. Guo, S. Lin, J. Gu, et al., Adv. Funct. Mater. 31 (2020) 5709–5721.
[56] S. Zhou, X. Yang, W. Pei, et al., J. Phys. Energy 3 (2020), doi:10.1088/2515-7655/abb6d1.
[57] G. Kresse, J. Furthmüller, Phys. Rev. B 54 (1996) 11169–11186.
[58] G. Kresse, J. Hafner, Phys. Rev. B 47 (1993) 558–561.
[59] J.P. Perdew, J.A. Chevary, S.H. Vosko, et al., Phys. Rev. B 46 (1992) 6671–6687.
[60] J.P. Perdew, Y. Wang, Phys. Rev. B 45 (1992) 13244–13249.
[61] L. Schimka, J. Harl, A. Stroppa, et al., Nat. Mater. 9 (2010) 741–744.
[62] J.H. Montoya, C. Tsai, A. Vojvodic, J.K. Nørskov, ChemSusChem 8 (2015) 2180–2186.
[63] C.Z. He, R. Wang, D. Xiang, et al., Appl. Surf. Sci. 509 (2020) 145392.
[64] R. Dronskowski, P.E. Bloechl, J. Phys. Chem. A 97 (1993) 8617–8624.
[65] J.K. Nørskov, J. Rossmeisl, A. Logadottir, et al., J. Phys. Chem. B 108 (2004) 17886–17892.
[66] H. Yang, C. He, L. Fu, et al., Chin. Chem. Lett. 32 (2021) 3202–3206.
[67] B. Yang, L. Li, Z. Jia, et al., Chin. Chem. Lett. 31 (2020) 2627–2633.
[68] L. Fu, R. Wang, C.X. Zhao, et al., Chem. Eng. J. 414 (2021) 128857.
[69] A.A. Peterson, F. Abild-Pedersen, F. Studt, et al., Energy Environ. Sci. 3 (2010) 1311–1315.
[70] M. Zhang, W. Wei, S. Zhou, et al., Energy Environ. Sci. 14 (2021) 1544–1552.
[71] J.R. Huo, J. Wang, H.Y. Yang, C.Z. He, J. Mol. Model. 27 (2021) 38.
[72] W. Li, Q. Jiang, D. Li, et al., Chin. Chem. Lett. 32 (2021) 2803–2806.

[73] X. Guo, S. Lin, J. Gu, et al., Adv. Funct. Mater. 31 (2020) 2008056.
[74] S. Qi, Y. Fan, L. Zhao, et al., Appl. Surf. Sci. 536 (2021) 147742.
[75] A.H. Woomer, D.L. Druffel, J.D. Sundberg, et al., J. Am. Chem. Soc. 141 (2019) 10300–10308.
[76] P.F. Sun, W.L. Wang, X. Zhao, J.S. Dang, Phys. Chem. Chem. Phys. 22 (2020) 22627–22634.
[77] X. Liu, Y. Jiao, Y. Zheng, et al., J. Am. Chem. Soc. 141 (2019) 9664–9672.
[78] X. Liu, Y. Jiao, Y. Zheng, S.Z. Qiao, ACS Catal. 10 (2020) 1847–1854.
[79] J. Rodriguez, Surf. Sci. 226 (1990) 101–118.
[80] Y. Guo, Z. Chen, W. Wu, et al., Appl. Surf. Sci. 455 (2018) 484–491.
[81] T. Bligaard, J.K. Nørskov, S. Dahl, et al., J. Catal. 224 (2004) 206–217.